nature portfolio

Peer Review File

Cathode chemomechanics controls Li metal solid-state battery performance under low stack pressures

Corresponding Author: Professor Paul Braun

This manuscript has been previously reviewed at another journal. This document only contains information relating to versions considered at Nature Communications.

This file contains all reviewer reports in order by version, followed by all author rebuttals in order by version.

Version 0:

Reviewer comments:

Reviewer #1

(Remarks to the Author)
This is a well-written account of a study designed to determine the effect of cathode volume changes on solid state cell behavior. I enjoyed reading it. The most intriguing conclusion is that a cathode designed to have minimal change during cell charge/discharge can influence void formation on the lithium anode. Here are a few questions for the authors, which they may want to address in a revised version of the paper.

1) The different behaviors of NMC and LCO upon charge (contraction for NMC, expansion for LCO) suggest that it may be possible to manage stresses by mixing together active materials in the composite cathode, so that overall stresses are minimized. Is this a viable approach? Likewise, would it be possible to mix together different particle morphologies of the same material, where, for example, 003 and 110 facets are dominant (depending on shape)?
2) On p. 3, lines 82-83, it is stated that lithium diffusion and de/intercalation kinetics of LCO are highly dependent on crystallographic orientation, yet the voltage profiles for the two cells containing LCO cathodes with different orientations shown in Figure 1c and e look very similar, although the stress responses are opposite, as expected. Below this sentence it is stated that 003-LCO gave a lower specific capacity, but this is somewhat obscured in Figures d and f, where the C/10 cycles are shown. Recommend using the same range in the x-axis to illustrate this more clearly.
3) Is there any possibility of changes in crystallite orientation under the high pressures used for the experiment in Figure 1? Were electrodes inspected after the experiment to make sure?
4) The labeling of figures and figure captions in the SI is inconsistent.
5) It's a little surprising to see that stresses for composite LCO rise higher upon charge than for the worst-case scenario 003-LCO. I would expect that the solid electrolyte, carbon etc. added to the composite electrode would have a diluting effect, unless a reaction occurs. Likewise, if particles in the composite electrode are randomly oriented (which might depend on morphology) that should have somewhat of a diluting effect as well.
6) Figure S10 shows formation cycles for two types of LCO electrodes in cells with LTO (zero-strain anodes). These show fairly large coulombic inefficiencies, yet the cycling data in S10c doesn't reflect this. Presumably the formation cycles were omitted. This should be stated.
7) Could authors give more detail about how the dense cathodes with different orientations were produced?

Reviewer #2

(Remarks to the Author)
Referee's Report
NCOMMS-25-14482-T
Title: Cathode chemomechanics controls Li metal solid-state 2 battery performance under low stack pressures

This paper investigates the chemomechanics of cathode materials and argues that stress generated in the cathode during charge/discharge can enhance the cycle life of all-solid-state batteries (ASSBs) under low external pressure. The analysis of

stress evolution in different crystallographic orientations of the cathode material during charge/discharge is systematic and logically structured. However, the claim that stress generated in the cathode directly suppresses void formation in the lithium metal anode seems to involve a logical leap. First, it is questionable whether the stress from the cathode is sufficiently large to suppress void formation in lithium metal. Additionally, lithium void formation is significantly influenced not only by external pressure but also by the interfacial adhesion between Li and the solid electrolyte (SE). Consequently, the surface characteristics of the lithium metal anode and solid electrolyte may play a more critical role than chemomechanical effects by the volumetric changes in the cathode. Since the authors did not use an anode interlayer, interpreting Li void failure behavior solely based on stress from the cathode without analyzing the surface conditions of the sulfide SE and lithium metal may be an overinterpretation. Moreover, the cathode/SE interface (solid-solid interface) is also crucial for the performance of ASSBs. The stress applied internally and externally to the cell can significantly impact the stability of this interface. The volume expansion/contraction behavior of the cathode, depending on its crystallographic orientation, may be more important for maintaining the cathode/SE interface than for lithium metal anode stability.
Since the correlation between cathode chemomechanical properties and lithium metal anode void formation is the most critical aspect of this paper, the current version does not appear suitable for publication in Nature Communications.

Please find my detailed comments below:
1. During discharge, lithium void formation is strongly influenced by the characteristics of the Li metal–solid electrolyte interface. Poor contact and impurities can lead to localized lithium stripping, resulting in void formation. Since the study does not use an anode interlayer, it is essential to first explain how the lithium metal–solid electrolyte interface was consistently controlled.
2. In Figure 2, the pressure difference caused by volume changes in the N-LCO cathode during charge/discharge is about 40 kPa. This value is relatively small compared to the external pressure (1 MPa–5 MPa) and the pressure induced by volumetric changes in the lithium metal anode. It is questionable whether this is sufficient to suppress lithium void formation, as the stress generated during Li metal plating/stripping is expected to be much higher.
3. The charge transfer reaction and Li diffusivity at the cathode interface may vary depending on the crystallographic orientation of the cathode material, influencing the overall electrochemical kinetics of the cell. In Figures 3 and 4, at a low C-rate (0.2C) where lithium voids do not form, the achievable capacity and impedance resistance differ depending on the cathode's crystallographic orientation. Thus, differences in cathode orientation may lead to variations in current distribution rather than stress, affecting lithium plating uniformity. The observed performance differences in low-pressure ASSBs could be attributed to variations in current uniformity rather than pressure effects.
4. In Figure 4, it is difficult to attribute the changes in high-frequency impedance solely to the Li-SE interface resistance. Charge-transfer reactions at the cathode-SE interface may also contribute to these variations in the high-frequency impedances.
5. The confocal profilometry results in Figure S15 appear to be evidence of non-uniform lithium plating rather than direct proof of void formation. Additional analysis, such as cross-sectional SEM or FIB-TEM of the lithium–solid electrolyte interface, is needed to directly confirm void formation.
6. The cathode–solid electrolyte interface is also a solid-solid contact, making it just as crucial for cell performance as the Li metal/SE interface. It appears more reasonable to argue that cathode chemomechanical properties have a more direct impact on maintaining the cathode/SE interface.
7. In Figure 6, the solid electrolyte content differs within the LCO and NMC composite cathodes. Differences in solid electrolyte content could affect the cathode/SE interface during cycling and lead to performance variations in ASSBs. Further clarification on this aspect is required.

Reviewer #3

(Remarks to the Author)
This manuscript presents a systematic and conceptually meaningful investigation into the role of cathode chemomechanics in Li metal solid-state batteries (SSBs), focusing on the influence of crystallographic orientation on interfacial stability under low stack pressure. The authors introduce a model system of LCO cathodes (P-, Z-, and N-LCO) with distinct lattice textures and connect their chemomechanical behavior to void formation and critical current density. The study is technically sound and offers a useful framework for thinking about compliant vs non-compliant interfaces (N-CAT vs P-CAT). However, there are several key issues that should be addressed before the work can be considered for publication. These include clarification on sample preparation, interpretation of composite electrode behavior, and the strength of claims regarding cycling stability and cathode stress classification.

1. The novelty of this study lies in using LCO samples with different textures to study stress behavior. However, the manuscript lacks detail on how the different textures (P-, Z-, N-LCO) were achieved. Please clarify which synthesis parameters were varied (e.g., plating, substrate, annealing) and how these led to the observed textures.

2. The (110) and (108) reflections in LCO are close in angle and may overlap in XRD. This raises concern about the accuracy of texture analysis. Please support the assignments with additional evidence (e.g., TEM or SAED).

3. The P-CAT label is applied to composite LCO cathodes, but it's unclear if they retain any texture. The methods describe composition, but not texture. If they are textured, please provide supporting data. If not, avoid classifying them as P-CAT.

4. N-LCO shows capacity fade over ~15 cycles, which is not discussed. P-LCO shows voiding but retains similar capacity. The manuscript should address whether N-LCO is clearly more stable and revise the use of 'remarkable stability' if not.

5. NMC shrinkage starts above ~4.2 V. Since 4.3 V was used, the N-CAT label might be valid. However, no quantitative volume change is shown. Please provide expected volume changes and explain the choice of voltage range.

6. Please clarify if stress measurements were repeated on multiple samples. Given the subtle stress signals, reproducibility is important. Report how many samples were tested and include any averaged results if available.

Version 1:

Reviewer comments:

Reviewer #1

(Remarks to the Author)
The authors have satisfactorily answered all the reviewers' questions. The paper is now ready for publication.

Reviewer #2

(Remarks to the Author)
The raised issues have been adequately addressed in the revised manuscript with supplementary data.

Reviewer #3

(Remarks to the Author)
The authors have adequately addressed all of my comments. The revisions have significantly improved the manuscript, and I recommend it for publication.

Author Responses to Reviewer Comments

We greatly appreciate the Reviewers' comments on our manuscript. We have carefully considered each of the recommendations and made revisions accordingly. Each of the Reviewer's comments requesting action on our part is listed below and is followed by our response and revisions. The Reviewer's comments are written in black italic font, our responses are in blue font and revisions to the manuscript are in red (revisions in the manuscript are highlighted in yellow).

Reviewer #1

1) The different behaviors of NMC and LCO upon charge (contraction for NMC, expansion for LCO) suggest that it may be possible to manage stresses by mixing together active materials in the composite cathode, so that overall stresses are minimized. Is this a viable approach? Likewise, would it be possible to mix together different particle morphologies of the same material, where, for example, 003 and 110 facets are dominant (depending on shape)?

Response: Jurgen Janek indeed showed that by mixing different active materials that one can control the collective chemomechanical response of the cathode just as the referee suggests.[1] A complication of this approach is that the onset voltage of each material can be different, resulting in a complicated electrochemical and chemomechanical response. We elected to conduct experiments with a single active material to enable a deeper understanding of the impact of cathode chemomechanics on full cell lithium metal solid-state battery performance.

Revisions: We added few sentences to the manuscript on page 7 stating "As shown by Janek et al., mixing cathode active materials with opposing chemomechanical behavior in solid-state batteries can control the collective chemomechanical response of the cathode.[2] However, differing onset voltages of materials can complicate electrochemical and chemomechanical responses. Hence, we focused our efforts on single active material to study the impact of cathode chemomechanics on full-cell lithium metal solid-state battery performance.", including the appropriate reference to highlight Janek's work and to note that minimizing overall stress, as we show using Z-LCO is not beneficial to prevent void formation at low stack pressures.

2) On p. 3, lines 82-83, it is stated that lithium diffusion and de/intercalation kinetics of LCO are highly dependent on crystallographic orientation, yet the voltage profiles for the two cells containing LCO cathodes with different orientations shown in Figure 1c and e look very similar, although the stress responses are opposite, as expected. Below this sentence it is stated that 003-LCO gave a lower specific capacity, but this is somewhat obscured in Figures d and f, where the C/10 cycles are shown. Recommend using the same range in the x-axis to illustrate this more clearly.

Response: We thank the reviewer for this suggestion. We have modified Figure 1 as requested.

Revisions: Modified Figure 1 is presented following.

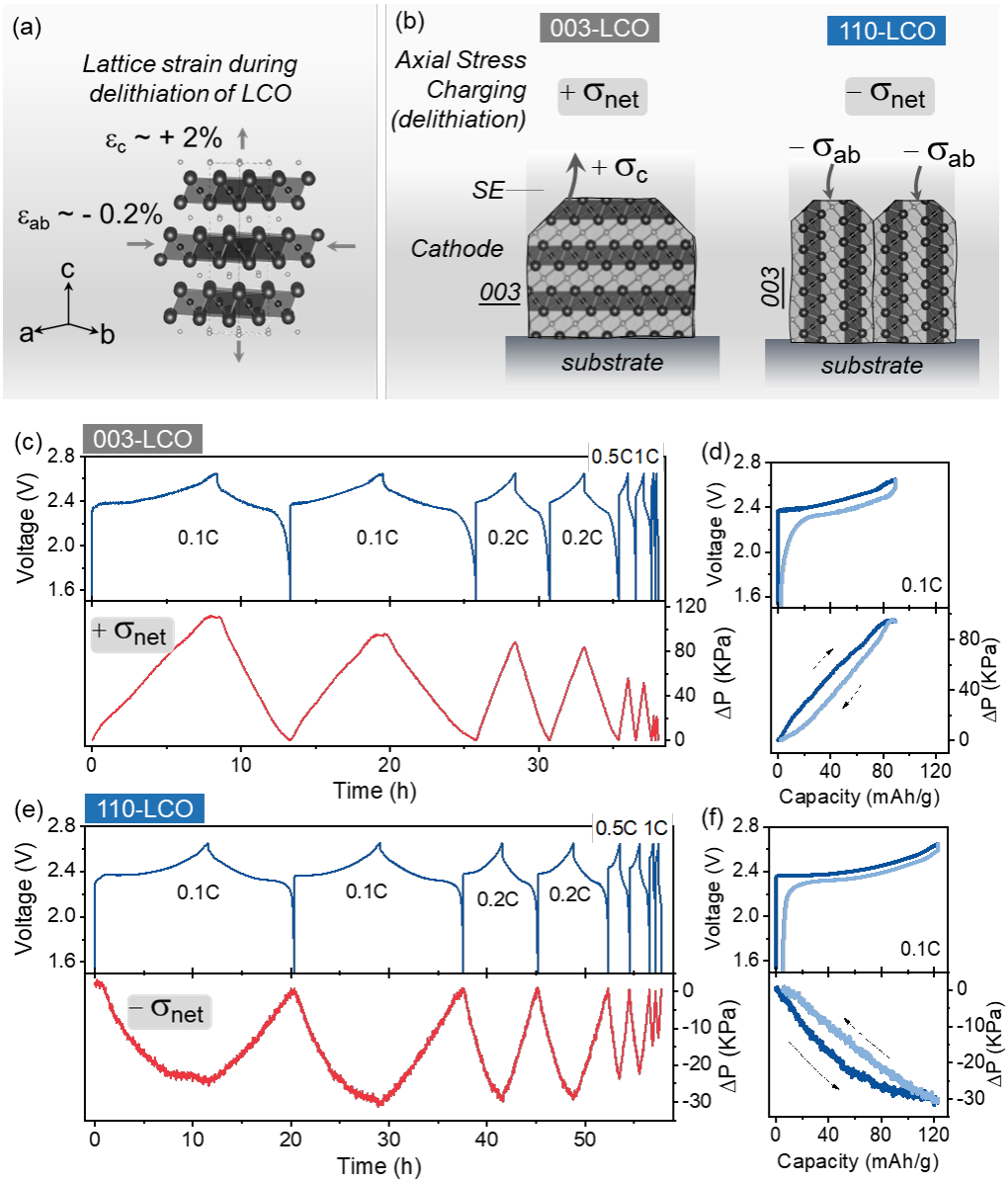

Figure 1 | Texture-dependent cathode chemomechanics. (a) Schematic representation of LCO lattice strain along c-axis and ab-plane during a typical charge (delithiation) to 4.2 V vs Li. (b) Schematic of cathode crystal orientation with respect to substrate based on microstructural analysis, (003) planes shown for reference. Axial pressure monitoring results for (c) 003-LCO and (e) 110-LCO at cycling rates of 0.1C, 0.2C, 0.5C and 1C in cell configuration of LCO|LIC|LYC|LTO/LYC at 26°C. The right panels (d and f) show reversible pressure response in the second 0.1C cycle. Stack pressure is 60 MPa, cathode loading is 1.2 mAh/cm^2.

3) Is there any possibility of changes in crystallite orientation under the high pressures used for the experiment in Figure 1? Were electrodes inspected after the experiment to make sure?

Response: We previously showed via cross-sectional FIB-SEM that textured LCO shows no changes in crystallite orientation under the high pressures used in the experiment (Figure R1 (a) and (b)). Figure R1 (a) shows the dense LCO before applying pressure, Figure R1 (b) shows the LCO after applying 360 MPa. There is no observable changes in crystallite orientation. These observations are in-line with our previously published studies[2,3] where before and after cross-sectional FIB-SEM as well as XRD analysis confirm the structure of LCO remains intact during cell fabrication.

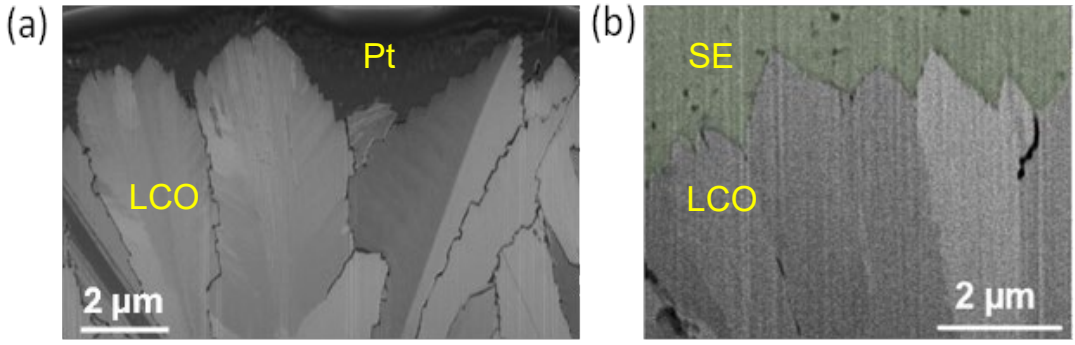

Figure R1. (a) SEM cross section of a textured LCO before pressing. (b) SEM cross section of a textured LCO after pressing LIC SE on the top surface (The green coloring of LIC is for illustration purposes).[2, 3]

Revision: To indicate fabrication pressure has no effect on the crystallite orientation of textured LCO, we added the following sentence to the main text, Methods section.: "The fabrication pressure applied to the textured LCOs in solid-state batteries caused no observable changes in crystallite orientation, as confirmed by our previously published cross-sectional FIB-SEM and XRD analyses".[3, 2]

4) The labeling of figures and figure captions in the SI is inconsistent.

Response: Thank you for pointing out the inconsistency in the labeling of figures and figure captions in the SI. We corrected this throughout the document.

5) It's a little surprising to see that stresses for composite LCO rise higher upon charge than for the worst-case scenario 003-LCO. I would expect that the solid electrolyte, carbon etc. added to the composite electrode would have a diluting effect, unless a reaction occurs. Likewise, if

particles in the composite electrode are randomly oriented (which might depend on morphology) that should have somewhat of a diluting effect as well.

Response: We also were surprised to observe that the stress in the composite LCO was greater than for 003-LCO as no carbon additives or binders were used in the fabrication of composite cathodes for stress measurements. To increase our confidence that reactions between SE and active material is not the reason for stress in the composite cathodes we subjected a cell to 4.5 V vs Li (exceeding LIC voltage stability of 4.2 V vs Li), as detailed in Figure S7 (g) and in the main text (page 7). This allowed us to systematically evaluate the impact of SE decomposition under controlled conditions and to observe that oxidation of the SE results in a minor reduction in volume, consistent with previous findings.[4, 5] The origin of this additional stress remains unclear. Perhaps it is due to the collective interaction of many granular particles changing in volume, but this is purely a speculation on our part.

Revisions: To highlight the larger stresses observed in the composite LCO compared to 003-LCO, we have added the following sentence to the main text (page 7): "The larger stresses observed in the composite LCO compared to 003-LCO are surprising, and perhaps result from the collective interaction of many active particles changing in volume embedded in an inactive medium."

6) Figure S10 shows formation cycles for two types of LCO electrodes in cells with LTO (zero-strain anodes). These show fairly large coulombic inefficiencies, yet the cycling data in S10c doesn't reflect this. Presumably the formation cycles were omitted. This should be stated.

Response: The Coulombic efficiency of formation cycles for plated LCO electrodes in cells with LTO anodes, as shown in Figure S10, ranges from 70% to 75%, depending on cycling protocols and operational conditions. The Reviewer's comment regarding the absence of formation cycle data in the capacity retention plot is correct. The cycling data in Figure S10 (c) does not reflect these inefficiencies because the formation cycle data were excluded, as the rate of cycling was changed to 0.5C during long-term cycling.

Revision: To clarify this, a statement has been added to the caption of the Figure S10 regarding "at 0.5C rate". Also we added the statement of "Cycling data shown excludes the initial formation cycle" to all figures presenting cycling data.

7) Could authors give more detail about how the dense cathodes with different orientations were produced?

Response: We appreciate your interest in the LCO production conditions. We first published the methodology used here in **Electroplating lithium transition metal oxides, Science Advances, 2017**,[6] and subsequently in additional publications.[3,6,7] For the referee's interest, here is an excerpt from reference (Nature Materials, 2021).[3] "Electroplated LCO was fabricated by Xerion Advanced Battery according to the process described in an earlier study[22]. In a typical synthesis, the electroplating bath was prepared by mixing KOH and LiOH with a weight ratio of 5:1 in an Ar-filled glove box. It was then heated at 260 °C until the mixture became transparent. About 2 wt% CoO was added into the melt, turning the solution blue due to the dissolved $Co(OH)_4^{2-}$ complex. A Co wire and a Ni plate were used as the reference and the counter electrodes, respectively. Al foil was used as the working electrode and substrate. The orientation of LCO was controlled by plating at low flux conditions near the oxidation onset (see cyclic voltammetry (CV) in ref. 22) for basal plane samples (Xerion product XABC_LCO_BP_1007595) and at high flux near peak oxidation for highly faceted samples (Xerion product XABC_LCO_HF_15195)."

Revisions: The following sentence was added on page 19. "Electroplated $LiCoO_2$ (LCO) was supplied by Xerion Advanced Battery Corp. (Kettering, OH), and was grown following published methodologies. [2,3,6,7]"

Reviewer #2

1) During discharge, lithium void formation is strongly influenced by the characteristics of the Li metal–solid electrolyte interface. Poor contact and impurities can lead to localized lithium stripping, resulting in void formation. Since the study does not use an anode interlayer, it is essential to first explain how the lithium metal–solid electrolyte interface was consistently controlled.

Response: We agree the lithium metal-solid electrolyte interface is important. To ensure consistent control of the Li metal anode preparation in this study, a lithium metal chip was manually rolled between two flat stainless steel surfaces inside an argon-filled glovebox (oxygen and moisture levels below 0.1 ppm), forming a shiny Li sheet with a thickness of 20-40 µm, as shown in Figure R2 (a). This Li sheet was rolled/fixed onto a thin copper foil (10 µm thick), and the resulting Li-laminated copper was punched into the required sizes (Figure R2 (b)). The freshly prepared Li metal anodes with copper current collectors were placed onto LPSC solid electrolyte (which is already densified with LIC SE layer and cathode electrode together under 500 MPa with a hydraulic pressing machine) and pressed under 25 MPa for 1 minute (as detailed at methodology section) (Figures R2 (c) and (d)). This process ensured uniform and consistent contact between Li metal and the LPSC solid electrolyte without the use of an interlayer. Additionally, we confirm that all LPSC powders and Li metal materials were used as purchased, with no modifications, and all cells in this study were assembled and tested using identical materials and brands to maintain consistency throughout the experiments. Furthermore, we provided multiple cell data (Figure R2 (e) and (f)) with same loading and current density to ensure consistency and reproducibility in the cells' fabrication and performance. Through our extended cell data validation, we paid particular attention to cell overpotential, impedance data (not shown here) and initial Coulombic efficiency to arrive at a consistent cell fabrication methodology.

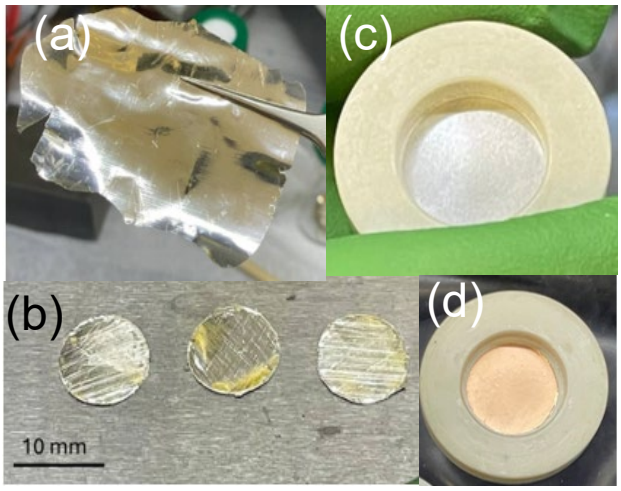

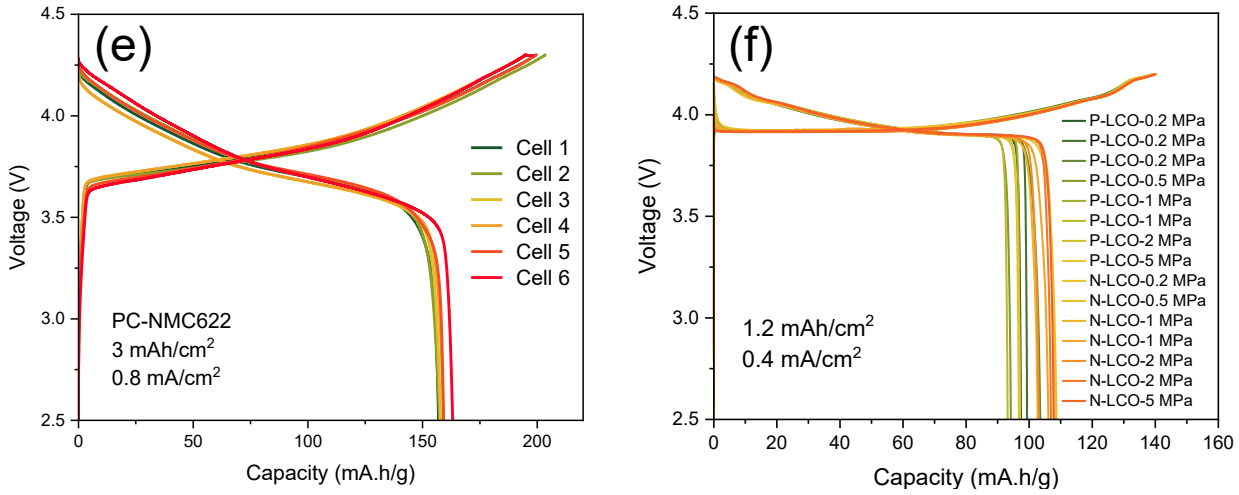

Figure R2. (a) Freshly rolled thin Li metal anode. (b) Punched Li metal pressed onto Cu current collectors. (c) The surface of a densified LPSC SE pallet inside a Ti-die cell without anode. (d) Pressed Li anode onto SE pallet surface. (e) Different PC-NMC622 cells' performance with a cell configuration of NMC/LPSC|LIC|LPSC|Li at 1 MPa and room temperature. (f) P-LCO and N-LCO cells' performance with a cell configuration of LCO|LIC|LPSC|Li at room temperature.

Revisions: The above plots have now been added to the SI as Figure S19, and a sentence describing the consistency of Li metal anode preparation is added to the Methods section. "Fig. S19 (e and f) illustrate the consistency in the Li-metal cells' fabrication and operations."

2) In Figure 2, the pressure difference caused by volume changes in the N-LCO cathode during charge/discharge is about 40 kPa. This value is relatively small compared to the external pressure (1 MPa–5 MPa) and the pressure induced by volumetric changes in the lithium metal anode. It is questionable whether this is sufficient to suppress lithium void formation, as the stress generated during Li metal plating/stripping is expected to be much higher.

Response: We agree the 40 kPa pressure difference induced by volume changes in the N-LCO cathode during charge/discharge (Figure 2), is small compared to the external stack pressures of 1 MPa to 5 MPa. This is perhaps why the community has not investigated the impact of cathode chemomechanics on voiding at the anode. Our data clearly shows there exists a coupling between cathode chemomechanics and anode voiding at low stack pressures. We note the effect of cathode chemomechanics is much more pronounced for 1 MPa stack pressure than for 5 MPa stack pressure. The direction of cathode chemomechanics clearly plays a critical role at low stack

pressures, further evidence that cathode chemomechanics is important to cell performance. We note our hypothesis that cathode chemomechanics is important at the anode is supported by optical profilometry (Fig. S15), which shows that the Li current collector remains flat after cycling against N-LCO, in contrast to the rough surface observed with P-LCO, and by cross-sectional FIB-SEM imaging (Fig. S16, a figure added in response to question 5 below), which confirms the absence of voids at the Li/SE interface in N-LCO cells, unlike in P-LCO and composite LCO cells. The totality of these observations indicates that the negative stress behavior of N-LCO, despite its modest 40 kPa contribution, effectively mitigates void formation.

As specific evidence of void formation when cathode chemomechanics is not appropriate, we now include detailed EIS analysis in a three-electrode cell to highlight the behavior of individual electrodes-SE interfaces for a P-LCO vs. Li cell. The new EIS is presented in Figures R3 (a-c). Figure R3 (a) (CE vs. Ref) shows that the Li anode side exhibits a significant impedance increase at the end of discharge under low stack pressure (1 MPa), attributed to increased contact loss, i.e., void formation at the Li/SE interface.

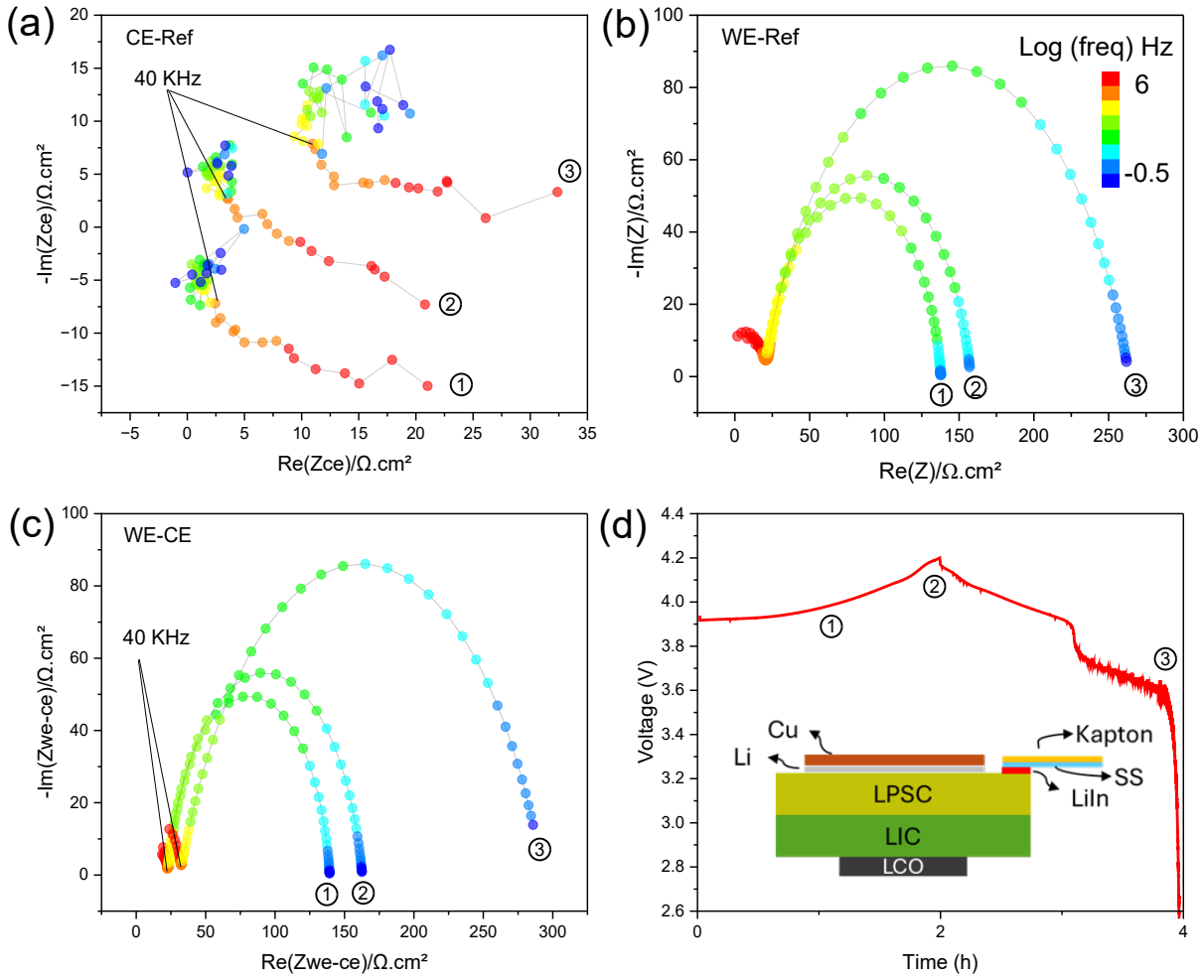

Figure R3. **Impedance analysis of a three-electrode cell under 1 MPa stack pressure for interfacial voiding mechanism studies. Nyquist plots depict intra-cycle impedance measurements for:** (a) Working Electrode (WE), (b) Counter Electrode (CE), and (c) Overall cell (WE-CE). (d) Corresponding charge/discharge data for P-LCO during void formation alongside with schematic of the three-electrode cell design, illustrating the configuration of WE, CE, and reference electrode (RE).

Revisions: The three-electrode cell data and cell configuration are added to the SI as Figure S21. Details of cell assembly have also been added to the Methods section on Page 20 as follows: "Three-electrode cell for EIS measurements was assembled similarly to textured LCO lithium metal cells. P-LCO was first pressed onto a double-layer LPSC/LIC SE from the LIC side at 500 MPa, followed by attaching a lithium anode with a Cu current collector onto the LPSC side. A stainless steel (SS) strip, bearing a small piece of indium metal and insulated with thin Kapton tape, was then pressed onto the LPSC SE alongside the lithium anode at 25 MPa (Fig. S21 (d)).

The In metal was lithiated using the Li anode as the counter electrode with 1 µA current for 1 hour."

3) The charge transfer reaction and Li diffusivity at the cathode interface may vary depending on the crystallographic orientation of the cathode material, influencing the overall electrochemical kinetics of the cell. In Figures 3 and 4, at a low C-rate (0.2C) where lithium voids do not form, the achievable capacity and impedance resistance differ depending on the cathode's crystallographic orientation. Thus, differences in cathode orientation may lead to variations in current distribution rather than stress, affecting lithium plating uniformity. The observed performance differences in low-pressure ASSBs could be attributed to variations in current uniformity rather than pressure effects.

Response: To address the Reviewer's concern regarding the role of cathodes orientation on the Li plating behavior, we conducted a statistical analysis of the overall performance of all cathodes. Data from multiple assembled cells using N-LCO, P-LCO, and Z-LCO cathodes (Figure R4) demonstrate no clear correlation between discharge capacity, cathode-SE resistance, and the specific type of cathode employed. This lack of correlation suggests that the electrochemical performance, in terms of capacity and resistance, does not significantly vary across these different LCO cathode types and all three cathodes, N-LCO, P-LCO, and Z-LCO exhibit nearly identical transport properties. This similarity suggests there are not substantial differences in current density distribution across the cathode-SE interface that would lead to uneven lithium plating at the anode side.

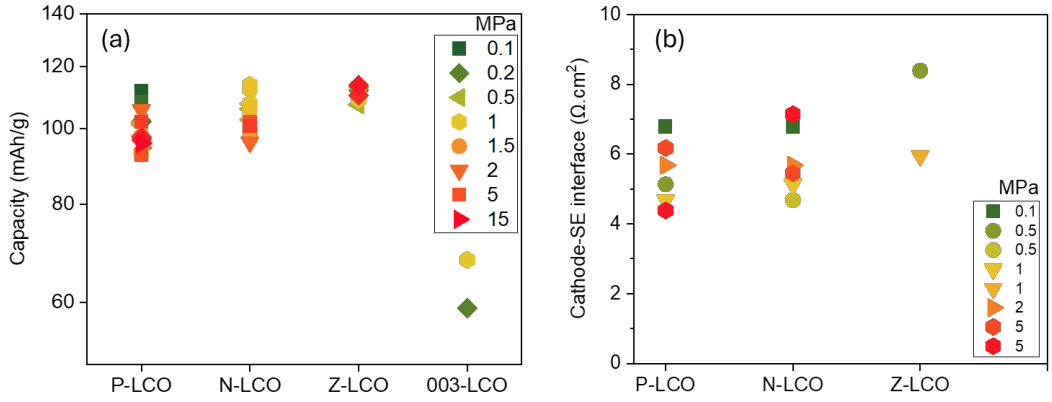

Figure R4. (a) Discharge capacities achieved for different types of LCO under different stack pressures. (b) Cathode/SE interfacial resistance for different cathodes at different stack pressures.

Further experiments with composite cathodes provide additional insight into the observed behaviors. Specifically, the NMC composite cathode, which generates negative stress during the charging process (similar to the behavior observed in N-LCO), does not show any evidence of voiding failure when cycled at a low pressure of 1 MPa and room temperature. In contrast, the composite LCO cathode, which generates stress in a manner comparable to P-LCO, is prone to void formation under the same conditions. These observations highlight a critical distinction between the two composite cathode materials despite their identical fabrication processes, which ensure consistent cathode-SE interfacial adhesion. The fact that composite LCO and NMC cathodes, with their differing chemomechanical behavior (such as stress generation during cycling), exhibit these contrasting behaviors underscores the broader applicability of our study's findings. It suggests that the trends observed are not limited to a single material system but are relevant across different cathode compositions.

Importantly, in the low SOC region of the cathode where voiding is observed in the cell comprised of composite LCO cathode (Figure 6 (a) in main text), its electronic and ionic conductivities are higher than those of the NMC composite cathode at similar SOC.[8,9,10] This difference implies that the formation of voids in the LCO system is not a result of sluggish cathode kinetics, such as limitations in charge transfer or lithium-ion diffusion at the cathode/SE interface. Instead, the higher conductivity of LCO during this SOC region suggests that the cathode is capable of supporting efficient charge and ion transport, ruling out cathode-related kinetic bottlenecks as the primary cause of voiding in this study.

Revisions: Figure R4 is added to the SI as Figure S20.

4) In Figure 4, it is difficult to attribute the changes in high-frequency impedance solely to the Li-SE interface resistance. Charge-transfer reactions at the cathode-SE interface may also contribute to these variations in the high-frequency impedances.

Response: The reviewer raises a valid point which motivated us to conduct additional detailed three-electrode solid-state battery testing. Our additional data provides a clearer picture of the mechanism of void formation under low stack pressure. Based on the analysis of the new three-

electrode cell EIS data (Figure R3, question 2) and Figure 4 of the main text, we can better elucidate the contributions to the high-frequency impedance variations (Figure R3 is re-presented below to avoid refering back and forth to few pages above). The EIS measurements were conducted at three distinct points during a cycle illustrated in Figure R3 (d) (1) middle of charge, (2) end of charge, and (3) end of discharge. Figure R3 (a) shows CE vs. Ref, representing the Li anode impedance; Figure R3 (b) shows WE vs. Ref, representing the cathode impedance; and Figure R3 (c) shows WE vs. CE, representing the overall cell impedance. The schematic of the three-electrode cell configuration, as shown in Figure R3 (d), consists of LCO as the cathode (WE), LPSC/LIC as double layer SE, and Li metal as the anode (CE). A LiIn alloy reference electrode is integrated within the LPSC electrolyte layer to enable precise potential measurements of the WE and CE separately. The LiIn alloy was chosen as the reference electrode due to its stable electrochemical potential of approximately 0.62 V vs. Li/Li^+, which provides a reliable reference point for measuring the individual potentials of the anode and cathode. Additionally, LiIn exhibits good stability in contact with sulfide-based solid electrolytes like LPSC, minimizing unwanted side reactions, and its relatively low impedance ensures accurate EIS measurements without significant interference.[11]

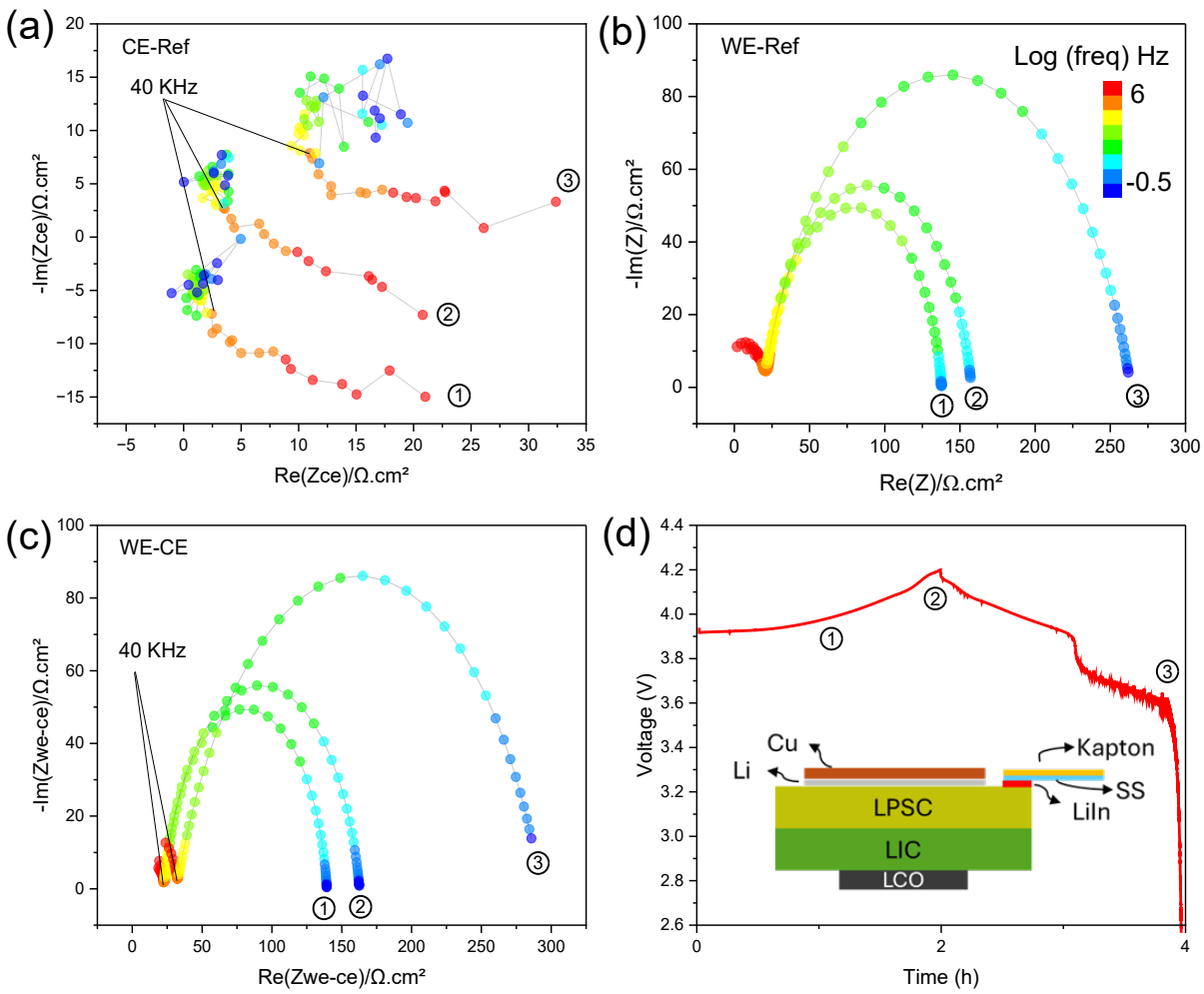

Figure R3. **Impedance analysis of a three-electrode cell under 1 MPa stack pressure for interfacial voiding mechanism studies. Nyquist plots depict intra-cycle impedance measurements for:** (a) Working Electrode (WE), (b) Counter Electrode (CE), and (c) Overall cell (WE-CE). (d) Corresponding charge/discharge data for P-LCO during void formation alongside with schematic of the three-electrode cell design, illustrating the configuration of WE, CE, and reference electrode (RE).

The EIS data in Figure R3 (a) (CE vs. Ref), which isolates the Li anode side, reveal that the impedance spectra remain stable throughout the charging process, with no significant shifts. However, at the end of discharge, a shifting towards higher impedance values is observed across the entire frequency range, including the high-frequency region. This shift, as depicted in Figure R3 (a), is indicative of void formation at the Li/ SE interface. Such voiding likely increases the interfacial resistance, contributing to the observed increase in high-frequency impedance.

In contrast, the EIS data in Figure R3 (b) (WE vs. Ref), which isolates the cathode side, show that the high-frequency region remains relatively stable throughout the cycling process. These panels display consistent high-frequency semicircles with minimal variation, indicating that the cathode/SE interface does not undergo significant changes in this frequency range. Instead, variations are primarily observed in the mid-frequency region, which can be attributed to changes in the cathode's SOC, as the semicircles shift in a manner consistent with SOC-dependent charge-transfer processes.[3, 12]

Consequently, while the cathode contributes to the overall EIS spectra in Figure R3 (c) (WE vs. CE), its influence is predominantly in the mid-frequency region rather than the high-frequency region. Figure R3 (c) highlights that the overall high-frequency impedance shift observed at the end of discharge can be primarily attributed to the anode side. The pronounced shift in the high-frequency region of the overall EIS data in Figure R3 (c) aligns with the changes observed in Figure R3 (a), reinforcing that the Li/SE interface degradation-specifically void formation-is the dominant factor driving the high-frequency impedance increase.

Revisions. The three-electrode cell data along with discussion above are now added to the SI. Also the method of fabrication is now added to the main text Methods Section. In Section 3.2., a sentence referring to this detialed three-electrode cell data in the SI is also added. "Three-electrode EIS data (SI section 10, Figure S21), confirms the assignment of each frequency region to a particular interface."

5) The confocal profilometry results in Figure S15 appear to be evidence of non-uniform lithium plating rather than direct proof of void formation. Additional analysis, such as cross-sectional SEM or FIB-TEM of the lithium–solid electrolyte interface, is needed to directly confirm void formation.

Response: Here we provide a brief explanation of our hypothesis on void formation along with new SEM-FIB cross-sectional data to support our hypothesis of the interplay between cathode chemomechanics and Li voiding at low stack pressure. Under low stack pressures and ambient temperature, conditions are favorable for void formation during the lithium stripping process in P-

LCO, Z-LCO and composite LCO cells. Voids formed during stripping can lead to non-uniform lithium plating in subsequent cycles, initiating a self-reinforcing cycle of uneven lithium distribution which manifests as large, island-shaped non-uniformities across the anode surface, which deform the Cu current collector. Previous studies of local distribution of Li plating and stripping have observed similar effects.[13,14,15] In the absence of sufficient external pressure, these deformations are irreversible. The confocal profilometry images from Figure S15 (P-LCO) reflect such anode deformations (including the Cu current collector) originating from voids formed during earlier stripping cycles in P-LCO cells. In contrast, N-LCO cells exhibit no such surface non-uniformities on the Cu current collector indicating uniform lithium plating and stripping processes.

To provide additional supporting data, we now include FIB-SEM cross-sectional images of the Li-LPSC interface from cells with different cathodes after an equivalent number of cycles with same operational conditions. As shown in Figure R5 (a) and (b), no void formation is observed at the Li/SE interface in N-LCO and composite NMC622 cells, after cycling at 1 MPa and room temperature. In contrast, voids are evident at the Li/SE interface in P-LCO and composite LCO cells, as depicted in Figure R5 (c) and (d).

Revisions: To address the need for direct evidence of void formation, we included cross-sectional FIB-SEM images (Figures R5 (c-d)) of the Li-LPSC interface in the SI as S16 (a-d). To clarify that these FIB-SEM results support the confocal profilometry findings, we have added the following sentence to the main text (page 10): "Moreover, cross-sectional FIB-SEM imaging of the Li-SE interface (Fig. S16) confirms the presence of voids in P-LCO and composite LCO cells."

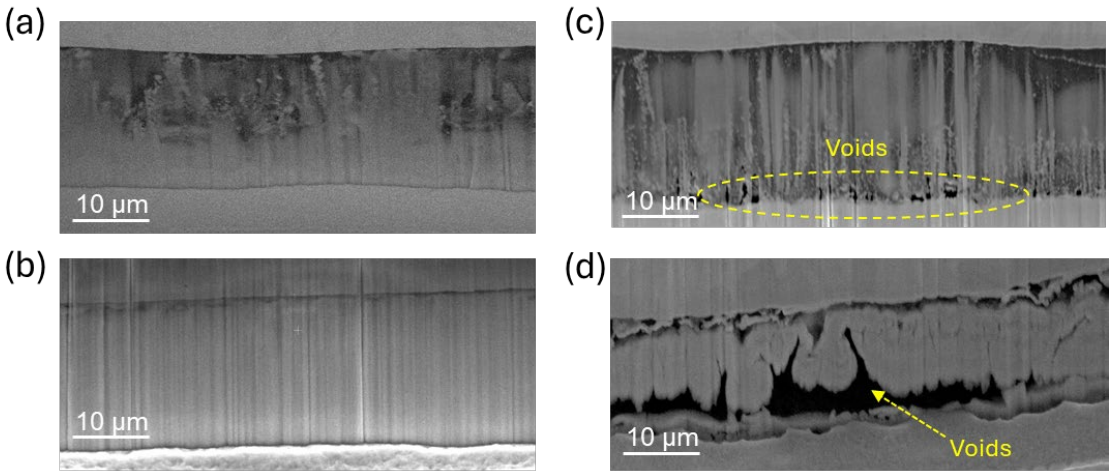

Figure R5. **FIB-SEM analysis of Li-LPSC interfaces with different cathodes after same number of cycles:** (a) N-LCO, showing a void-free Li-SE interface. (b) Composite NMC622 cathode, presenting a stable, void-free Li-SE interface. (c) P-LCO, displaying void formation at the Li-SE interface. (d) Composite LCO cathode, exhibiting voids at the interface. Images represent typical interfacial morphology under 1 MPa stack pressure, highlighting cathode-dependent voiding behavior.

6) The cathode–solid electrolyte interface is also a solid-solid contact, making it just as crucial for cell performance as the Li metal/SE interface. It appears more reasonable to argue that cathode chemomechanical properties have a more direct impact on maintaining the cathode/SE interface.

Response: We acknowledge the Reviewer's point regarding the important role of the cathode-SE interface on cell performance. Our data appears to rule out an effect of cathode chemomechanics on the cathode/SE interface in our system. Most importantly, EIS data (Figure 4 (c, e) (main text) illustrates the stability of the cathode-SE interface for both N-LCO and P-LCO cathodes. Our new statistical analysis of a collection of dense cathode data (presented in Figure R4, Figure S20 in the revised manuscript) confirms the stability of cathode/SE interface under different stack pressure and orientation. Cross-sectional FIB-SEM images (Figure R5) from our prior study on the cathode/SE interface[3] demonstrate good adhesion, with no evidence of voiding or delamination, between various textured LCO cathodes and the LIC after cycling.

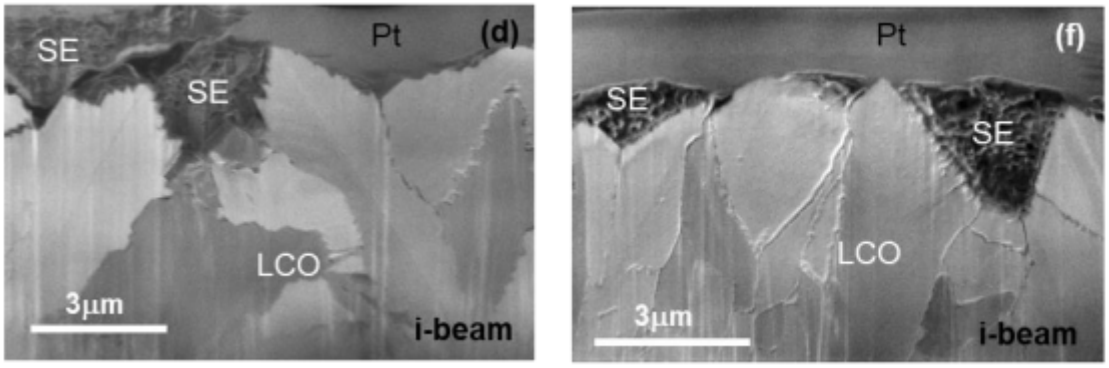

Figure R5. **FIB-SEM cross section of dense LCOs-SE interface:** Two dense LCO cathodes with distinct textures showing a stable LCO-SE interface without delamination or voiding signs after cycling. (reproduced from our previous work.[3])

Revisions: To confirm the stability of the cathode-solid electrolyte interface, we have added Figure R4 to the SI as Figure S20 as well as the following sentence to the main text on page 10: " Moreover, statistical analysis (SI section 10, Figure S20), and cross-sectional FIB-SEM images from the prior study confirm that the transport properties of the three types of cathodes, P-LCO, Z-LCO and N-LCO remain similar and intact before and after cycling. Three-electrode EIS analysis (SI section 10, Figure S21 also confirms the SOC-dependent interfacial resistance behavior of cathode-SE interface.[3]" supported by our EIS data (Figure R3), statistical analysis (Figure R4), and prior cross-sectional FIB-SEM (Figure R5) observations.

7) In Figure 6, the solid electrolyte content differs within the LCO and NMC composite cathodes. Differences in solid electrolyte content could affect the cathode/SE interface during cycling and lead to performance variations in ASSBs. Further clarification on this aspect is required.

Response: We appreciate the Reviewer's comment regarding the potential impact of differing SE content in the LCO and NMC composite cathodes on the cathode/SE interface and cycling performance. To address this concern, we now prepared an additional LCO composite cathode with the same composition as the NMC cathode (70% LCO, 27% SE, 3% carbon additive) and evaluated its electrochemical performance under identical testing conditions. The results (Figure R6) revealed no significant differences in cycling performance, capacity retention, or cathode/SE interface stability compared to the original LCO cathode (80:18:2) presented in Figure 6(a) of the

main text. Notably, the voiding behavior observed at the anode side under high current density remained consistent, indicating that the variation in SE content within the investigated range does not substantially influence the Li/SE interface. Furthermore, the overall cycling performance, including Coulombic efficiency and capacity retention, showed no significant changes. This insensitivity to SE content variations may be attributed to the inherently high electronic and ionic conductivity of LCO particles, which render the LCO cathode less dependent on SE and electronically conductive additives compared to NMC cathodes. These findings have been incorporated into the revised SI (Figure S18), as well.

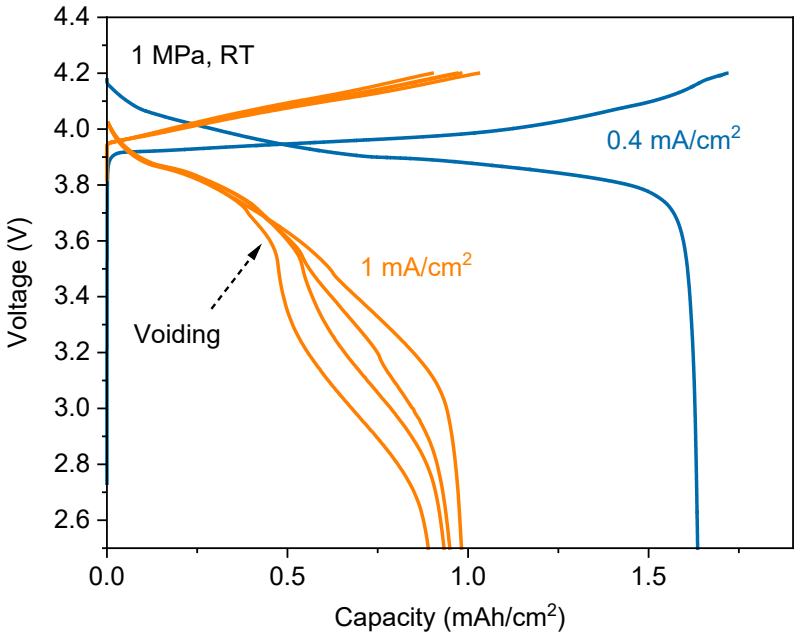

Figure R6. **Composite cathode Li metal SSBs.** LCO composite cathode cycled at "safe" (0.4 – 0.5 mA/cm^2) current density in first cycle and then at higher current density (1 mA/cm^2) in consecutive cycles.

Revisions: Figure R6 is added to the SI as Figure S18.

Reviewer #3

1) The novelty of this study lies in using LCO samples with different textures to study stress behavior. However, the manuscript lacks detail on how the different textures (P-, Z-, N-LCO) were achieved. Please clarify which synthesis parameters were varied (e.g., plating, substrate, annealing) and how these led to the observed textures.

Response: Reviewer #1 asked a similar question (question 7). Please see our detailed response regarding the LCO synthesis conditions above. To answer the specific question regarding the orientation here is an excerpt from our recently published J. Mater. Chem A paper.[7] "To obtain films with different textures, the growth temperature was controlled between 300 and 350 °C. Higher temperature results in the (003) basal planes lying parallel to the substrate, whereas lower temperature leads to the basal planes lying perpendicular to the substrate. At intermediate temperature (325 °C), a mixed orientation sample containing crystals lying in both the aforementioned orientations can be obtained. The deposited sample thickness is controlled with the deposition time.".

Revisions: The following sentence was added on page 19. "Electroplated $LiCoO_2$ (LCO) was supplied by Xerion Advanced Battery Corp. (Kettering, OH), and was grown following published methodologies. [2,3,6,7]" .

2) The (110) and (108) reflections in LCO are close in angle and may overlap in XRD. This raises concern about the accuracy of texture analysis. Please support the assignments with additional evidence (e.g., TEM or SAED).

Response: We understand the Reviewer's concern regarding overlapping 110 and 108 reflections. We conducted extensive XRD and high resolution STEM and diffraction analysis of these cathodes in our previous work[3] to confirm the assignment of Bragg reflections in our XRD analysis. A copy of this TEM analysis is extracted from Figure S3 of our previous work[3] here for the Reviewer's perusal (Figure R7).

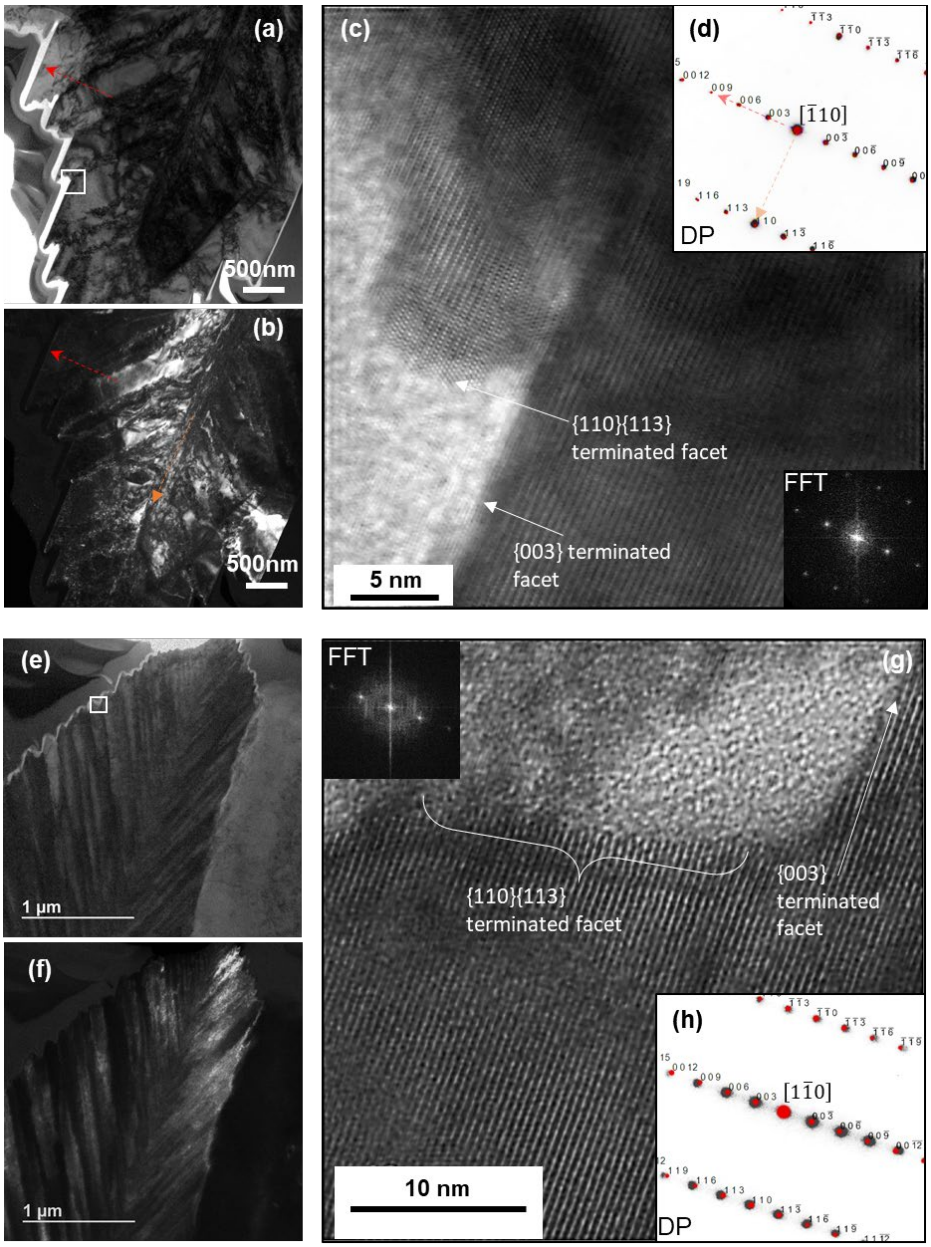

Figure R7 (Extracted from Ref [4].) TEM (bright and dark filed), high resolution micrographs and SAED patterns of (a-d) HF LCO and (e-h) PF LCO samples prepared via FIB. The central core and corresponding growth direction <110> are shown by orange dashed arrow. Simulated diffraction pattern overlaid on measured pattern (CrystalMaker). {003} planes are shown by red dashed arrow in (a,b). Dark field micrographs were collected using g = $(003)_{LCO}$ reflection.

We also note that the XRD peak separation between 108 and 110 is evident in our prior work's [3] XRD analysis of powder vs. plated LCO (Figure S5 of in Ref [4]) confirms the absence of the 108 peak in the plated LCO.

3) The P-CAT label is applied to composite LCO cathodes, but it's unclear if they retain any texture. The methods describe composition, but not texture. If they are textured, please provide supporting data. If not, avoid classifying them as P-CAT.

Response: We acknowledge the potential confusion. The P-CAT label is used to categorize cathodes based on their chemomechanical behavior, volume expansion during charge (delithiation) and the associated pressure response, as measured and illustrated in Figure 2 (h) and Figure 5 (d). This classification encompasses a range of LCO cathode types, including textured P-LCO, randomly oriented LCO powders, and randomly oriented high-voltage (HV) LCO powders, all of which exhibit positive pressure responses during charge. To reduce the possibility of confusion, we have made the revisions noted below.

Revisions: We have added these clarifications to the manuscript:
(Page 12): P-CAT denotes cathodes exhibiting positive stress during charge (delithiation), such as P-LCO and composite LCOs, whereas N-CAT refers to cathodes with negative stress during delithiation, such as N-LCO and composite NMCs.
(Methods section): "Randomly oriented LCO (Sigma Aldrich) and NMC (MSE Supplies) powders were used as received."

4) N-LCO shows capacity fade over ~15 cycles, which is not discussed. P-LCO shows voiding but retains a similar capacity. The manuscript should address whether N-LCO is clearly more stable and revise the use of 'remarkable stability' if not.

Response: We thank the Reviewer for highlighting the need for additional discussion regarding the cycling performance of N-LCO and P-LCO cathodes in Figure 5 (b, c), as well as the use of the term "remarkable stability." The terms "stable cycling" and "remarkable cycling stability" in section 3.3 refer to the N-LCO cathode's capacity retention of 86% over ~100 cycles in Figure 5 (c) under a current density of 0.75 mA/cm^2, in contrast to P-LCO (Figure 5 (a)). This comparison clarifies that N-LCO demonstrates greater stability against voiding.

Furthermore, to provide a more comprehensive analysis of P-LCO's (textured LCO) behavior, we include additional data here (Figure R8) illustrating the consistent voiding failure mechanism in Li-metal SSBs with P-LCO cathodes under 1 MPa stack pressure at room temperature. These data reinforce the distinct chemomechanical challenges associated with P-LCO compared to N-LCO. To ensure precision, we have also moderated the use of "remarkable stability" throughout the manuscript, reserving it for cases where cycling performance is exceptional and replacing it with more specific descriptors (e.g., "improved voiding resistance") where appropriate.

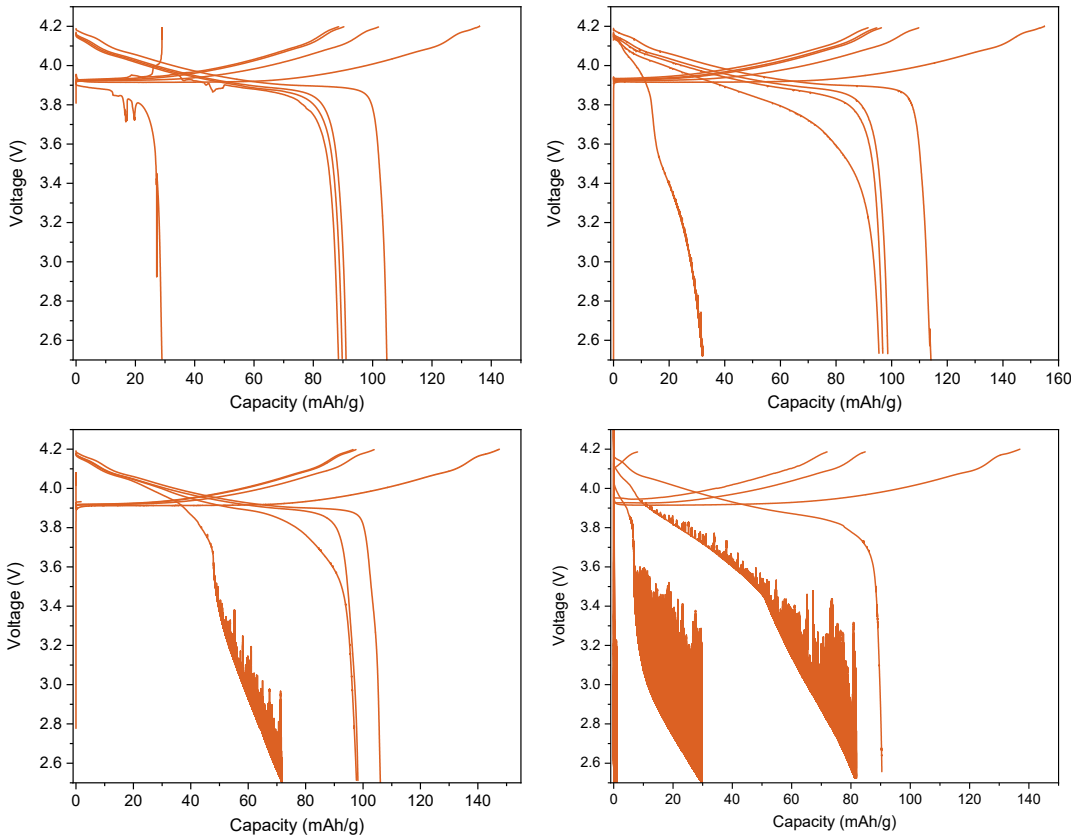

Figure R8. Multiple trials of evaluating the cycling performance of P-LCO (textured electroplated LCO with positive stress during charge) cathodes in Li-metal SSBs under same operational condition (1 MPa and room temperature at 0.5 mA/cm^2). All cells show signs of voiding behavior within few cycles.

Revisions: The term "remarkable stability" in section 3.3 replaced with "improved voiding resistance".

5) NMC shrinkage starts above ~4.2 V. Since 4.3 V was used, the N-CAT label might be valid. However, no quantitative volume change is shown. Please provide expected volume changes and explain the choice of voltage range.

Response: The voltage ranges for the cathode materials in this study were selected to maximize discharge capacity while ensuring the electrochemical stability of both the active materials and the solid electrolytes. For NMC the electrochemical stability extends to 4.4 V or even 4.5 V against lithium metal in solid-state systems, depending on the specific composition and crystallinity type (single crystal or polycrystal). To avoid particle-level cracking, which can occur at higher voltages due to anisotropic lattice strain and volume changes, an upper cutoff voltage of 4.3 V was selected for PC-NMC622 and 4.5 V for SC-NMC622. The choice of 4.3 V and 4.5 V aligns with the observation that NMC begins to exhibit significant volume shrinkage above approximately 4.2 V during delithiation (charge), as noted in the comment (note there is some volume shrinkage even below 4.2 V).[1,16]

For NMC622, the lattice undergoes approximately 1.6% contraction in the a,b-axes and 0.5% expansion in the c-axis when charged to 4.3 V Vs Li^+, resulting in a net unit cell volume contraction of approximately 1.5% to 1.7%.[1, 17] Charging to 4.5 V vs Li^+ would result in 3 to 4% volume changes in NMC622 unite cell.[1]

Revisions: We added the following statements regarding the voltage cut-off selection and volume change for each cathode to the Methods Section. "The voltage ranges for NMCs were selected to maximize capacity while ensuring structural stability, balancing the 1.5–1.7% volume change for both single-crystalline and polycrystalline NMC622 at 4.3 V vs. Li/Li^+ and the 3–4% volume change at 4.5 V vs. Li/Li^+.[1] Long-term cycling of SC-NMC622 was conducted within a voltage range of 2.5 V–4.5 V to achieve higher capacity while maintaining its structural stability at the particle level, whereas PC-NMC622 was cycled within 2.5 V–4.3 V due to its reduced structural stability beyond 4.3 V"

6) Please clarify if stress measurements were repeated on multiple samples. Given the subtle stress signals, reproducibility is important. Report how many samples were tested and include any averaged results if available.

Response: We conducted stress measurements on multiple cathodes to ensure reproducibility. We have added two new figures (Figures R9 (a) and (b) illustrating repeated stress measurements on N-LCO (replicating Fig. S4.b) and NMC622 (replicating Fig. S6 (e)).

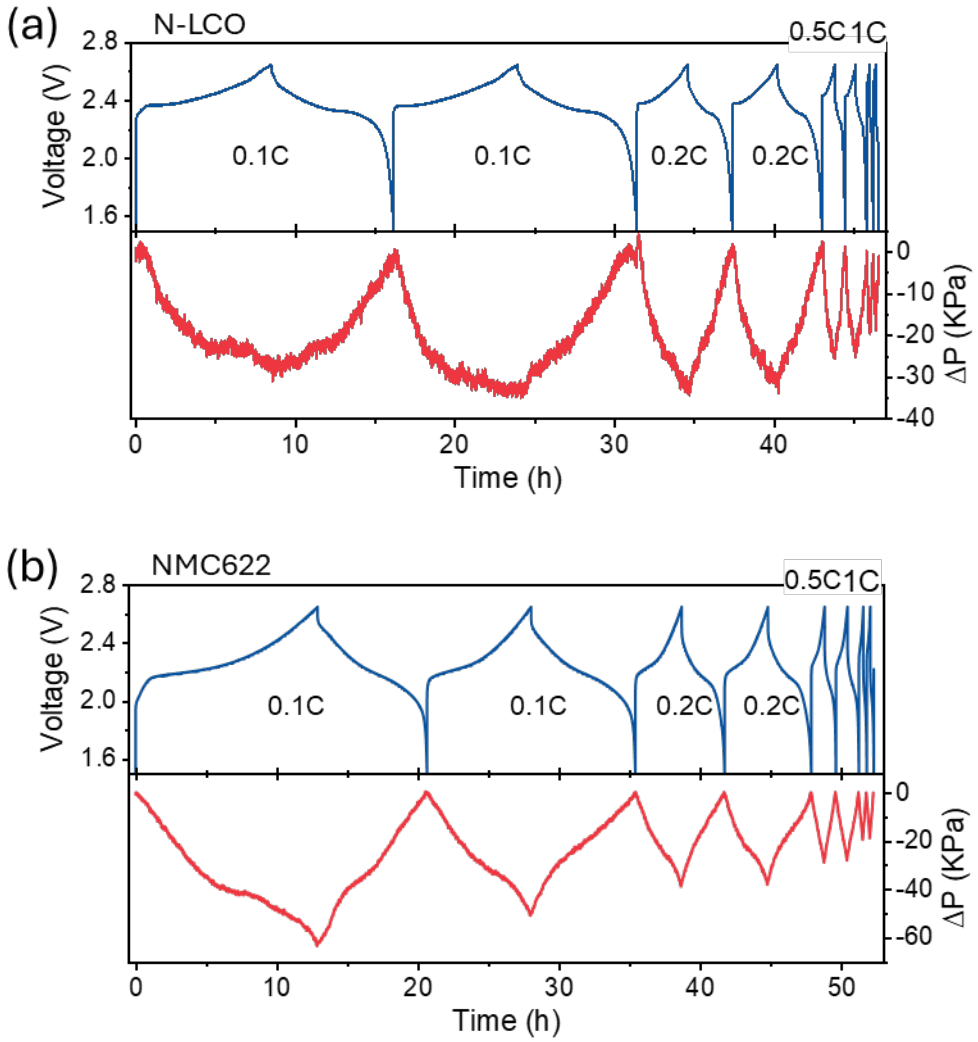

Figure R9. Axial pressure monitoring results for (a) N-LCO, (b) NMC622 at cycling rates of 0.1C, 0.2C, 0.5C and 1C in cell configuration of LCO|LIC|LYC|LTO/LYC and NMC/LIC|LIC|LYC|LTO/LYC at 26.6°C and 60 MPa respectively. Cathodes loading is 1.2 mAh/cm^2.

Revisions: Figure R9 is added to the SI as Figure S22.

References

(1) Koerver, R.; Zhang, W.; de Biasi, L.; Schweidler, S.; Kondrakov, A. O.; Kolling, S.; Brezesinski, T.; Hartmann, P.; Zeier, W. G.; Janek, J. Chemo-Mechanical Expansion of Lithium Electrode Materials – on the Route to Mechanically Optimized All-Solid-State Batteries. *Energy Environ. Sci.* **2018**, *11* (8), 2142–2158. https://doi.org/10.1039/C8EE00907D.

(2) Kwon, P. J.; Juarez-Yescas, C.; Jeong, H.; Moradi, S.; Gao, E.; Lawrence, D.; Zahiri, B.; Braun, P. V. Chemo-Electrochemical Evolution of Cathode-Solid Electrolyte Interface in All-Solid-State Batteries. *ACS Energy Lett.* **2024**, 4746–4752. https://doi.org/10.1021/acsenergylett.4c02062.

(3) Zahiri, B.; Patra, A.; Kiggins, C.; Yong, A. X. Bin; Ertekin, E.; Cook, J. B.; Braun, P. V. Revealing the Role of the Cathode–Electrolyte Interface on Solid-State Batteries. *Nat. Mater.* **2021**, *20* (10), 1392–1400. https://doi.org/10.1038/s41563-021-01016-0.

(4) Han, Y.; Hoo Jung, S.; Kwak, H.; Jun, S.; Kwak, H. H.; Hoon Lee, J.; Hong, S.-T.; Seok Jung, Y. Single-or Poly-Crystalline Ni-Rich Layered Cathode, Sulfide or Halide Solid Electrolyte: Which Will Be the Winners for All-Solid-State Batteries? **2021**. https://doi.org/10.1002/aenm.202100126.

(5) Wang, S.; Tang, M.; Zhang, Q.; Li, B.; Ohno, S.; Walther, F.; Pan, R.; Xu, X.; Xin, C.; Zhang, W.; Li, L.; Shen, Y.; Richter, F. H.; Janek, J.; Nan, C. W. Lithium Argyrodite as Solid Electrolyte and Cathode Precursor for Solid-State Batteries with Long Cycle Life. *Adv. Energy Mater.* **2021**, *11* (31), 2101370. https://doi.org/10.1002/AENM.202101370.

(6) Zhang, H.; Ning, H.; Busbee, J.; Shen, Z.; Kiggins, C.; Hua, Y.; Eaves, J.; Davis, J.; Shi, T.; Shao, Y. T.; Zuo, J. M.; Hong, X.; Chan, Y.; Wang, S.; Wang, P.; Sun, P.; Xu, S.; Liu, J.; Braun, P. V. Electroplating Lithium Transition Metal Oxides. *Sci. Adv.* **2017**, *3* (5). https://doi.org/10.1126/SCIADV.1602427/SUPPL_FILE/1602427_SM.PDF.

(7) Lin, J. W.; Xie, D.; Jeong, H.; Littlefield, A. J.; Spila, T.; Zahiri, B.; Braun, P. V. Role of Crystallographic Orientation in Atom Probe Analysis of Li-Ion Battery Cathode Materials. *J. Mater. Chem. A* **2025**, *13* (15), 10910–10919. https://doi.org/10.1039/D5TA00728C.

(8) McClelland, I.; Booth, S. G.; Anthonisamy, N. N.; Middlemiss, L. A.; Pérez, G. E.; Cussen, E. J.; Baker, P. J.; Cussen, S. A. Direct Observation of Dynamic Lithium Diffusion Behavior in Nickel-Rich, LiNi0.8Mn0.1Co0.1O2 (NMC811) Cathodes Using

Operando Muon Spectroscopy. *Chem. Mater.* **2023**, *35* (11), 4149–4158. https://doi.org/10.1021/ACS.CHEMMATER.2C03834/ASSET/IMAGES/LARGE/CM2C03834_0007.JPEG.

(9) Lakhdar, Y.; Chen, Y.; Geary, H.; Houck, M. E.; Groombridge, A. S.; Slater, P. R.; Kendrick, E. Toward Higher-Power Li-Ion Batteries: Unravelling Kinetics and Thermodynamics of MoNb12O33 vs. NMC622. *J. Power Sources* **2023**, *588*, 233710. https://doi.org/10.1016/J.JPOWSOUR.2023.233710.

(10) Van Der Ven, A.; Ceder, G. Lithium Diffusion in Layered Li x CoO 2. *Electrochem. Solid-State Lett.* **2000**, *3* (7).

(11) Chang, G. H.; Choi, H. U.; Kang, S.; Park, J. Y.; Lim, H. T. Characterization of Limiting Factors of an All-Solid-State Li-Ion Battery Using an Embedded Indium Reference Electrode. *Ionics (Kiel).* **2020**, *26* (3), 1555–1561. https://doi.org/10.1007/S11581-019-03367-W/TABLES/1.

(12) Zhang, W.; Weber, D. A.; Weigand, H.; Arlt, T.; Manke, I.; Schröder, D.; Koerver, R.; Leichtweiss, T.; Hartmann, P.; Zeier, W. G.; Janek, J. Interfacial Processes and Influence of Composite Cathode Microstructure Controlling the Performance of All-Solid-State Lithium Batteries. *ACS Appl. Mater. Interfaces* **2017**, *9* (21), 17835–17845. https://doi.org/10.1021/acsami.7b01137.

(13) Kazyak, E.; Wang, M. J.; Lee, K.; Yadavalli, S.; Sanchez, A. J.; Thouless, M. D.; Sakamoto, J.; Dasgupta, N. P. Understanding the Electro-Chemo-Mechanics of Li Plating in Anode-Free Solid-State Batteries with Operando 3D Microscopy. *Matter* **2022**, *5* (11), 3912–3934. https://doi.org/10.1016/J.MATT.2022.07.020.

(14) Thorpe, M. A.; Zhang, M.; Liao, D. W.; Sandoval, S. E.; Kim, Y.; McDowell, M. T.; Thouless, M. D.; Dasgupta, N. P. Controlling Stack Pressure Inhomogeneity in Anode-Free Solid-State Batteries Using Elastomeric Interlayers. *Matter* **2025**, *8* (3). https://doi.org/10.1016/j.matt.2024.101955.

(15) Sandoval, S. E.; Haslam, C. G.; Vishnugopi, B. S.; Liao, D. W.; Yoon, J. S.; Park, S. H.; Wang, Y.; Mitlin, D.; Hatzell, K. B.; Siegel, D. J.; Mukherjee, P. P.; Dasgupta, N. P.; Sakamoto, J.; McDowell, M. T. Electro-Chemo-Mechanics of Anode-Free Solid-State Batteries. *Nat. Mater.* **2025**, *24* (5), 673–681. https://doi.org/10.1038/S41563-024-02055-Z;TECHMETA=128;SUBJMETA=166,299,301,639,891,988;KWRD=BATTERIES,ME

CHANICAL+ENGINEERING.

(16) Reimers, J. N.; Dahn, J. R. Electrochemical and In Situ X-Ray Diffraction Studies of Lithium Intercalation in Li x CoO2. *J. Electrochem. Soc.* **1992**, *139* (8), 2091–2097. https://doi.org/10.1149/1.2221184/XML.

(17) Gu, J.; Liang, Z.; Shi, J.; Yang, Y.; Gu, J.; Liang, Z.; Shi, J.; Yang, Y. Electrochemo-Mechanical Stresses and Their Measurements in Sulfide-Based All-Solid-State Batteries: A Review. **2022**. https://doi.org/10.1002/aenm.202203153.